ORIGINAL ARTICLE

Exosomal proteomics identifies RAB13 as a potential regulator of metastasis for HCC

Xiu-Yan Huang[1] | **Jun-Tao Zhang**[2] | **Feng Li**[3] | **Ting-Ting Li**[4] | **Xiang-Jun Shi**[1] | **Jin Huang**[5] | **Xin-Yu Huang**[1] | **Jian Zhou**[6] | **Zhao-You Tang**[6] | **Zi-Li Huang**[1,7]

[1]Department of General Surgery, Shanghai Jiao Tong University Affiliated Sixth People's Hospital, Shanghai, PR China

[2]Institute of Microsurgery on Extremities, Shanghai Jiao Tong University Affiliated Sixth People's Hospital, Shanghai, PR China

[3]School of Materials of Science and Engineering, Shanghai Jiao Tong University, Shanghai, PR China

[4]Department of Infectious Disease, Shanghai Jiao Tong University Affiliated Sixth People's Hospital, Shanghai, PR China

[5]Department of Pathology, Shanghai Jiao Tong University Affiliated Sixth People's Hospital, Shanghai, PR China

[6]Liver Cancer Institute and Zhongshan Hospital, Fudan University, Shanghai, PR China

[7]Department of Radiology, Xuhui District Central Hospital of Zhongshan Hospital, Fudan University, Shanghai, PR China

Correspondence
Xiu-Yan Huang, Department of General Surgery, Shanghai Jiao Tong University Affiliated Sixth People's Hospital, 600 Yi Shan Road, Shanghai 200233, PR China.
Email: xyhuang1119@163.com

Abstract

Background: Exosomal proteins from cancer cells are becoming new biomarkers for cancer monitoring and efficacy evaluation. However, their biological function and molecular mechanism underlying tumor metastasis are largely unknown.

Methods: Bioinformatic methods such as bulk gene expression analysis, single-cell RNA sequencing data analysis, and gene set enrichment analysis were employed to identify metastasis-associated proteins. The *in vitro* and *in vivo* experiments were used to investigate the function of RAB13 in HCC metastasis.

Results: We identified RAB13 as one of the critical regulators of metastasis in HCC-derived exosomes for the first time. *In vitro*, the invasiveness of HCC cell lines could be attenuated by *RAB13* silence. *In vivo*, tumor size and proportion of high-grade lung metastatic nodule could be reduced in the mice with orthotopic transplantation of tumors and intravenously injected with exosomes derived from MHCC97H cell with RAB13 silence (si-RAB13-Exo), as compared with those without RAB13 silence (si-NC-Exo). Moreover, in si-RAB13-Exo

---

Z.L.H. is co-corresponding author.

Abbreviations: CPTAC, Clinical Proteomic Tumor Analysis Consortium; CTC, circulating tumor cell; GEO, Gene Expression Omnibus; HCC, hepatocellular carcinoma; HE, hematoxylin and eosin; IHC, Immunohistochemistry; MVD, microvessel density; TCGA, the Cancer Genome Atlas; TME, tumor microenvironment; PCA, principal component analysis; UMAP, Uniform Manifold Approximation and Projection.

Supplemental Digital Content is available for this article. Direct URL citations appear in the printed text and are provided in the HTML and PDF versions of this article on the journal's website, www.hepcommjournal.com.

- -

group, circulating tumor cell counts were decreased at the third, fourth, and fifth weeks after orthotopic transplantation of tumors, and MMP2 (matrix metalloproteinase 2)/TIMP2 (tissue inhibitor of metalloproteinases 2) ratio was also significantly decreased. In addition, RAB13 expression was also associated with VEGF levels, microvessel density, and tube formation of vascular endothelial cells by both *in vitro* and *in vivo* models, indicating that RAB13 was associated with angiogenesis in HCC.

Conclusions: We have demonstrated exosomal RAB13 as a potential regulator of metastasis for HCC by *in silico*, *in vitro*, and *in vivo* methods, which greatly improve our understanding of the functional impact of exosomal proteins on HCC metastasis.

INTRODUCTION

Liver cancer is estimated to be responsible for 8.3% of cancer death globally in 2020.[1] Basically, HCC often develops in a complex tumor microenvironment (TME) affected by chronic inflammation, which ultimately result in its poor prognosis.[2]

The TME, characterized by its acidic, hypoxic, and high-interstitial pressure nature, is mainly composed of extracellular matrix (ECM), fibroblasts, immune cells, mesenchymal stem cells, vessels, and other signaling molecules.[3,4] Of note, the TME interacts with tumor cells in diverse manners. Besides direct cell-to-cell contact, they also communicate through indirect ways including paracrine signaling by cytokines, growth factors, and extracellular vesicles.[5] The imbalance between the proteolytic activity of matrix metalloproteinase 2 (MMP2) and the tissue inhibitor of matrix metalloproteinase 2 (TIMP2) has been reported to be responsible for the degradation of ECM components,[6] and ECM degradation and re-modeling are required for the intravasation of tumor cells,[7] which play a key role in tumor invasion and metastasis. Exosomes are extracellular vesicles originating from early endosomes,[8] and along with microvesicles and apoptotic vesicles, exosomes are essential players in intercellular communications in the TME.[9,10] Cancer-derived exosome cargos often contain nucleic acids and proteins that help initiate a neoplastic microenvironment in multiple cancer types, as is reported.[11] Meanwhile, exosomal levels of specific noncoding RNAs and proteins could serve as indicators in the detection of a malignant tumor and/or metastasis.[12] Our previous work has demonstrated that exosomal circRNA-100338 could promote HCC metastasis by enhancing invasiveness and angiogenesis.[13] Due to the significant heterogeneity of exosomes, there are varied mechanisms behind exosome-mediated tumor metastasis. For example, exosomal EPHA2 derived from breast cancer cells promotes angiogenesis and metastasis,[14] suggesting that functional molecules carried by the tumor-derived exosomes played key roles in tumor metastasis. Generally, tumor-derived exosomes can regulate the sloughing of tumor cells from the primary sites, increase circulating tumor cell (CTC) count and promote metastasis.[15–17]

We have previously found that the low invasiveness of Hep3B could be enhanced by the co-culture with the exosomes derived from MHCC97H, an HCC cell line with highly metastatic potential, which give us a hint that some substances, such as DNAs, RNAs, or proteins, carried by tumor-derived exosomes might promote tumor cell metastasis. In this study, we found that RAB13, which could sustain the stemness of breast cancer cells by supporting tumor-stroma cross-talk,[18] was closely associated with pulmonary metastasis of HCC by bioinformatic analysis. To our knowledge, the functional role of RAB13 or exosomal RAB13 in HCC has not been unveiled by previous research studies so far. Therefore, we investigated the impact of RAB13 or exosomal RAB13 on HCC metastasis by *in silico*, *in vitro*, and *in vivo* methods, and anticipated to uncover the underlying mechanism of RAB13 in HCC metastasis.

MATERIALS AND METHODS

Patients, clinical specimens, and follow-up

The inclusion criteria for 10 consecutive HCC patients with advanced stage in this study were: (a) tumor node metastasis classification (TNM, IIIc–IV); (b) availability of specimens including CTCs, frozen biopsy, and/or resected primary and metastatic HCC tissues; (c) pathologically proven HCC based on World Health Organization (WHO) criteria; and (d) availability of clinical data. This study was approved by the ethics committee of our hospital (No. 2022-020; China Clinical Trial Registration Center—Registration No. ChiCTR220055847). The Written consent was obtained from all subjects.

Cell lines

HCC cell lines of MHCC97H and HCCLM3 with high metastatic potential were established at the authors' institution, and HCC cell line of Hep3B with very low invasiveness was purchased from Shanghai Cell Bank of the Chinese Academy of Sciences. The details for the cell culture can be seen in Supplementary Methods (http://links.lww.com/HC9/A14).

Mice grouping and treatments

Male athymic BALB/c nu/nu mice of 18–20 g at 5 weeks' age were obtained from the Shanghai Institute of Materia Medica, Chinese Academy of Science. All mice were handled according to the recommendations of the National Institutes of Health Guidelines for Care and Use of Laboratory Animals. Human HCC tumor models produced by MHCC97H were established in nude mice by orthotopic inoculation,[13] with some modifications. Thirty-six nude mice randomized into 2 groups were used in this study. Intravenous injection started on 2 hours after tumor implantation. si-NC-exo group (control group, $n = 18$): Each mouse received caudal vein injection of 100 μg exosomes (1 μg/μL) derived from si-NC-MHCC97H cells. si-RAB13-Exo group [knockdown (KD) group, $n = 18$]: Each mouse received caudal vein injection of 100 μg exosomes (1 μg/μL) derived from si-RAB13-MHCC97H cells. Three nude mice in each group were randomly sacrificed by cervical dislocation and autopsied 48 hours after injection at the end of the 0, first, second, third, fourth, and fifth week. Tumor volume was estimated by the formula $V = \pi/6 \times a \times b^2$, where a was the long and b was the short tumor axis, and pulmonary metastasis was examined by hematoxylin and eosin staining at the fifth week. The degree of lung metastasis was graded by the maximum number of tumor cells counted in the solitary pulmonary metastatic nodules (grades): grade I, $n < 20$; grade II, $n = 20$–50; grade III, $n = 50$–100; grade IV, $n > 100$.[19] Pulmonary metastatic extent was defined as low grade (I, II) and high grade (III, IV).

Samples prepared

Culture supernatants, blood samples, lung tissues, tumor tissues, and protein extracts were harvested for *in vitro* and *in vivo* studies.

Proteomic data analysis of HCC cell line-derived exosomes

The protein intensity of the HCC cell line-derived exosomes was downloaded from PRIDE database with accession PXD004779.[20] The details can be seen in Supplementary Methods (http://links.lww.com/HC9/A14).

Single-cell RNA sequencing (scRNA-seq) data analysis

The count table of scRNA-seq data was downloaded from Gene Expression Omnibus (GEO) with accession GSE125449.[21] Among the 19 tumor samples, 9 HCC samples were used and 10 intrahepatic cholangiocarcinoma samples were excluded in this study. The data preprocessing and normalization was conducted by R Seurat package.[22] Specifically, the cells with low quality were excluded if the gene counts were smaller than 200 or greater than 3000, or the percent of unique molecular identifier count mapped to mitochondrial genes was above 20%. The count was normalized by being divided by the total counts for that cell and multiplied by the scale factor ($1e^6$). The principal component analysis was conducted based on the top 2000 variable genes. Moreover, the multiple samples were integrated by R Harmony package.[23] The Uniform Manifold Approximation and Projection (UMAP) reduction was conducted on the PCs by Harmony. The single cells were clustered by a shared nearest neighbor modularity optimization-based clustering algorithm at the resolution of 0.5, and clusters with the same marker genes were merged as the same cell type. The marker genes for the cell types were obtained from the previous study.[21] The Multi-subject Single Cell deconvolution (MUSIC) method was employed to estimate the cell proportions using bulk RNA sequencing data.[24]

Gene set enrichment analysis

The gene set enrichment analysis was implemented by R clusterProfiler package.[25] Specifically, the enrichment of pathway genes in the differentially expressed genes/proteins was tested by the Fisher exact test (using the *enricher* function). The enrichment of CUX1 target genes in the upregulated genes of RAB13-hi malignant cells/HCC cell models was conducted by gene set enrichment analysis (using *GSEA* function).

Quantitative Real-time PCR

Total RNA was prepared using TRIzol reagent (Invitrogen) following the guidance. The complementary DNA was synthesized by 5xTransScript All-in-One SuperMix and used for quantitative PCR analysis following the manufacturer's instructions, respectively. The complementary DNA samples were diluted to 10% concentration and used as templates for quantitative PCR analysis (ABI Stepone plus). The primer sequences for RAB13 are listed as follows:

Forward primer: TCCATGCAGAATTTTCGTCACC.
Reverse primer: TACTAGGATAATGCCCATGGCT.

Western blot

The proteins were first isolated from the cells using RIPA lysis buffer. Subsequently, the isolated proteins were quantified by the BCA assay kit (Beyotime Biotechnology). Each 40 μg total protein was electrophoresed on 10% SDS-polyacrylamide gel and then transferred to polyvinylidene fluoride membranes, which were incubated with primary antibodies against RAB13 (Abcam; ab233810). A secondary antibody was added and incubated for 2 hours at 37°C. Glyceraldehyde 3-phosphate dehydrogenase gene products were used as the internal controls for both RNA and protein quantification.

KD of RAB13 gene

The small interfering RNA (siRNA) sequences targeting RAB13 were designed according to a modified Tuschel standard, and the detailed siRNA sequences were as follows:

si-RAB13: (+) 5′- TGACCTCAACTACATGGTC-TACA-3′, (−) 5′- CTTCCCATTCTCGGCCTTG-3′.

The details can be seen in Supplementary Methods (http://links.lww.com/HC9/A14).

Stable lentiviral transfection of HCC cells

HCC cells were plated in 24-well plates. Subconfluent cells were infected with 3 mL/well 3 times (3 hours per infection). The cells were divided into 2 groups: the KD cells transfected with RAB13 siRNA lentivirus (KD group), and the negative control cells transfected with empty lentivirus (normal control group).

RAB13 overexpression

The full sequence of RAB13 was amplified by the standard PCR procedure. We transfected the pCMV6-empty and pCMV6-RAB13 into Hep3B cancer cells and RNA was extracted. RAB13 overexpression was confirmed, and invasive potential was assessed.

Isolation of exosomes from culture supernatants

Isolation of exosomes in supernatants according to our previous study,[13] with some modifications. Exosomes were resuspended in precooled PBS and examined by transmission electron microscope.

Nanoparticle tracking analysis

The study used a ZetaView particle tracker (ParticleMetrix) to detect the concentration and size of exosomes. In brief, 1 mL sterile PBS was used to resuspend the exosomes, and then exosomes were injected into a clean sample pool. Next, the sample tool was placed into the instrument to detect the size of the exosomes for further volume distribution analysis.

Isolation and identification of CTCs in blood samples

The CTCs in blood samples were isolated and identified following the previous report,[26] with some modifications. The details can be seen in Supplementary Methods (http://links.lww.com/HC9/A14).

Immunohistochemistry (IHC) assay

Intratumoral microvessels immunostained for CD34 (Abcam; ab269304) were counted using the method described by the earlier study.[27] The details can be seen in Supplementary Methods (http://links.lww.com/HC9/A14).

ELISA

Protein levels of MMP2, TIMP2, and VEGF in the serum-free supernatants of HCC cell lines and in the tumor tissue extracts were measured via commercially available MMP2 (R&D Systems), TIMP2 (Amersham Biosciences), and VEGF ELISA (R&D Systems) kits. Absorbance was measured at 450 nm, using a microplate spectrophotometer with the correction wavelength of 570 nm. The assays were conducted in triplicate.

Cell proliferation and invasion assays

The CCK8 kit (Absin; abs50003) was used to measure the cell proliferation levels. The cell invasion assays were conducted in triplicate using transwell chambers (8 μm pore size; Millipore) and chambers coated with Matrigel,[19] respectively. The details can be seen in Supplementary Methods (http://links.lww.com/HC9/A14).

Tube formation assay

Tube formation assay was performed to assess the effect of exosomal RAB13 on angiogenesis. Growth factor-reduced Matrigel (BD Biosciences) was placed in 48-well plates. Human umbilical vein endothelial cells (HUVECs) were first incubated with serum-free medium

for 12 hours and then transferred onto the 48-well plates precoated with Matrigel. After incubation for 10 hours, tube formation was examined in photographs taken under a microscope. The total tube length was determined by measuring the branches of blood vessels using ImageJ software.

Statistical analysis

The 2-sample comparison was tested by t test. The contingency table was tested by chi-square test. p value < 0.05 was considered as statistically significant.

RESULTS

Identification of proteins associated with metastasis from HCC-derived exosomes

Our previous work found that the invasive ability of Hep3B could be enhanced by co-culture with the exosomes of MHCC97H.[13] In this study, we further observed that invaded cells of MHCC97H could be increased about 15.5% by co-culture with the exosomes of HCCLM3 (baseline vs. co-culture groups, 35.2 ± 3.9 vs. 40.7 ± 4.8, Figure 1A, $p = 0.0018$), giving us a hint that some substances, such as DNAs, RNAs, or proteins, carried by tumor-derived exosomes might promote tumor cell metastasis. Therefore, to identify the proteins associated with HCC metastasis from tumor-derived exosomes, we re-analyzed the protein abundances in exosomes derived from 3 HCC cell lines, including Hep3B, MHCC97H, and HCCLM3, by the previous study.[20] Specifically, the differential protein abundance analysis was conducted by comparing the exosomes derived from HCC cells of highly metastatic potential (MHCC97H and HCCLM3) with those of lowly metastatic potential (Hep3B). Totally, we identified 31 and 61 proteins with higher abundance in the exosomes derived from HCC cell lines with highly and lowly metastatic potential, respectively (Figure 1B, adjusted p < 0.15, p < 0.05, fold change > 2). Interestingly, the proteins involved in complement cascade were highly abundant in the exosomes derived from both HCC cell lines with lowly metastatic potential (A2M, SERPINA1, F2, FGG, FGA, C4BPB, C3, FGB) and those with highly metastatic potential (CFHR1, CFH, and C1S) (Figure 1C, D). Moreover, MET, one of receptor tyrosine kinases, and RAB13, one of *RAS* oncogene family members, were also observed to be highly abundant in the exosomes of HCC cell lines with highly metastatic potential (Figure 1D). These results suggested that the proteins with higher abundance in the exosomes of HCC cell lines with highly metastatic potential might be implicated in the HCC metastasis.

RAB13 is highly expressed in malignant cells and associated with poor prognosis

To further screen out the exosomal proteins associated with HCC metastasis, we investigated the expression levels of genes encoding the metastasis-associated proteins within exosomes in HCC malignant cells and tissues. The scRNA-seq data analysis (16,498 single cells and 9 HCC samples) identified 7 major cell types (Figure 2A, B), including B cells (*MS4A1*, *CD79A*, and *CD79B*), hepatic stellate cells (*RGS5*, *PDGFRB*, and *ACTA2*), T cells (*CD3D*, *CD3E*, and *CD3G*), myeloid cells (*LYZ*, *AIF1*, and *CD14*), endothelial cells (*KDR*, *VWF*, *PLVAP*), natural killer cells (*KLRC2*, *KLRF1*, and *KLRC3*), and malignant cells (*ALB*, *GPC3*, and *AFP*). Notably, the genes encoding RAB13, CFHR1, AKR1C4, CFH, C1S, MET, and AGR2 were highly expressed in malignant cells of HCC tissues (Figure 2C and Figure S1, http://links.lww.com/HC9/A9). Among those genes, *RAB13* and *MET* were found to be upregulated in HCC tissues as compared with the adjacent normal tissues using 3 public gene expression datasets (The Cancer Genome Atlas, GSE14520, and CPTAC) (Figure 2C and Figure S2, http://links.lww.com/HC9/A10). The protein expression levels of both RAB13 and MET were also upregulated in HCC tissues, as compared with the adjacent normal tissues (Figure 2C, CPTAC cohort). As MET has been well studied by previous studies,[28,29] we then focused on the functional role of RAB13 in HCC metastasis. Even though *RAB13* was expressed in both malignant cells and endothelial cells, its RNA expression level was significantly higher in malignant cell than endothelial cell (Figure 2D). Furthermore, higher expression of *RAB13* was associated with shorter overall survival in the 3 HCC cohorts (Figure 2E). These results suggested that high expression of *RAB13* in malignant cells might be associated with poor prognosis.

RAB13 silence in MHCC97H could attenuate exosome-induced invasion in Hep3B via the decrease of MMP2/TIMP2 ratio

As the protein abundance of RAB13 was higher in the exosomes of HCC cell lines with highly metastatic potential, we then employed western blot assay to quantify its expression levels in HCC cell lines. Consistently, RAB13 was expressed highest in HCCLM3, followed by MHCC97H and Hep3B (Figure 3A), suggesting that RAB13 was associated with the metastatic potential in HCC. We have previously found that the exosomes derived from HCC cell lines with highly metastatic potential (MHCC97H) could enhance the invasiveness of cells with lowly metastatic potential (Hep3B).[13]

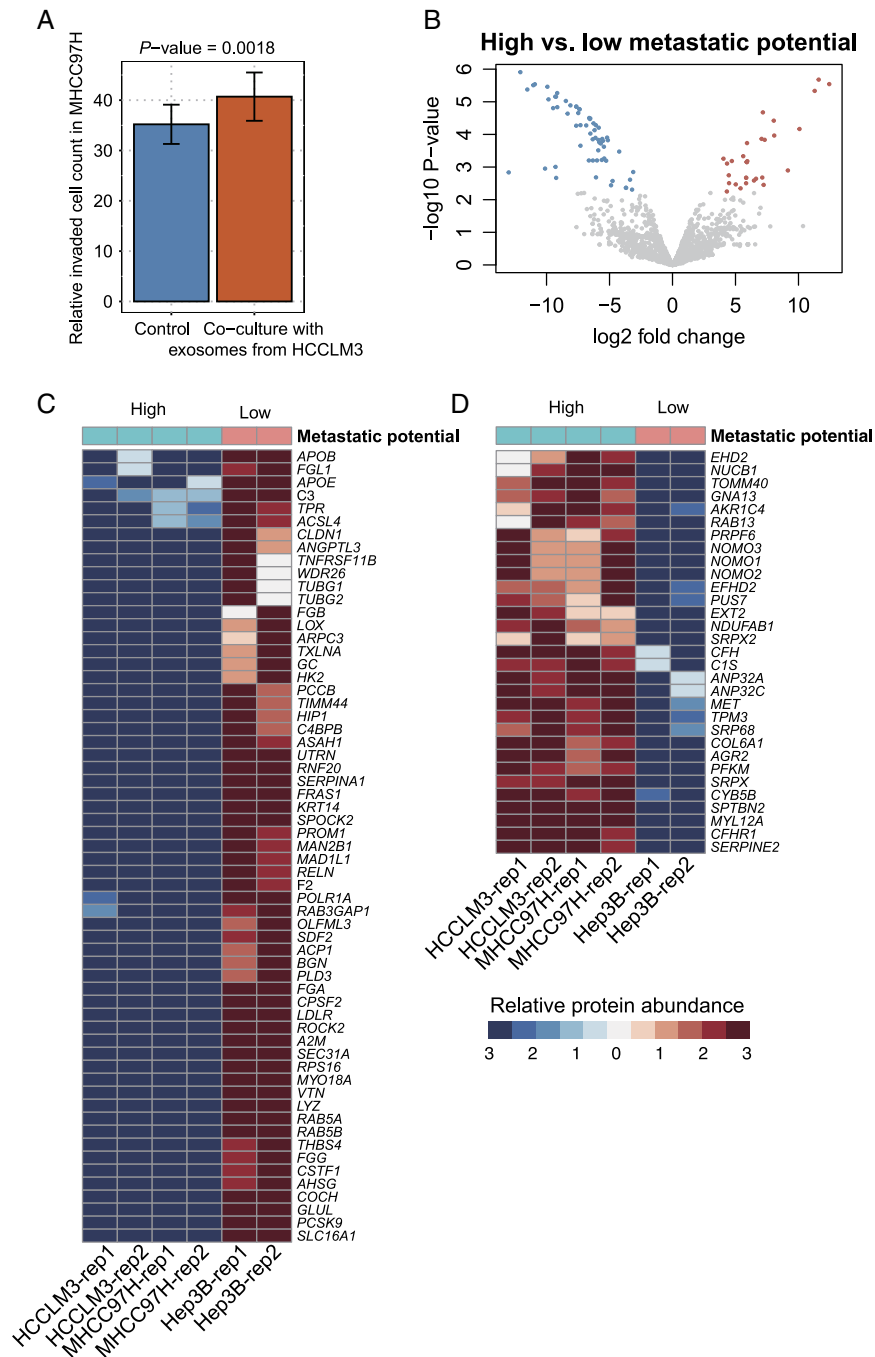To explore the association of RAB13 with HCC invasion, we KD RAB13 expression in the highly

FIGURE 1 The differential abundance of exosomal proteins between HCC cell lines with highly and lowly metastatic potential. (A) The number of invaded cells in MHCC97H with and without co-culture of the exosomes derived from HCCLM3. (B) The volcano plot for the exosomal proteins with differential abundance. The red and blue points represent the highly and lowly abundant proteins in the exosomes of HCC cell lines with highly metastatic potential. The proteins with low and high abundance in the exosomes of HCC cell lines with highly metastatic potential were displayed in (C) and (D).

metastatic cell line (MHCC97H) by siRNAs, and overexpressed RAB13 expression in the lowly metastatic cell line (Hep3B). The decreased expression of *RAB13* RNA in the si-RAB13-MHCC97H indicated that KD could efficiently suppress *RAB13* RNA expression (a decrease of 54.0% of RAB13 expression in si-RAB13, $p < 0.001$). Accordingly, the increased expression of RAB13 RNA in the OE-RAB13-Hep3B

suggested that the overexpression could increase RAB13 expression (an increase of 10.2 folds of *RAB13* RNA expression in OE-RAB13, $p < 0.001$). A significant decrease of invaded cells was observed in MHCC97H with si-RAB13 treatment [control (si-NC) vs. RAB13 KD (si-RAB13), 36.4 ± 4.1 vs. 28.9 ± 5.3, $p < 0.001$, Figure 3B]. The RAB13 overexpression in Hep3B significantly enhanced its invasiveness
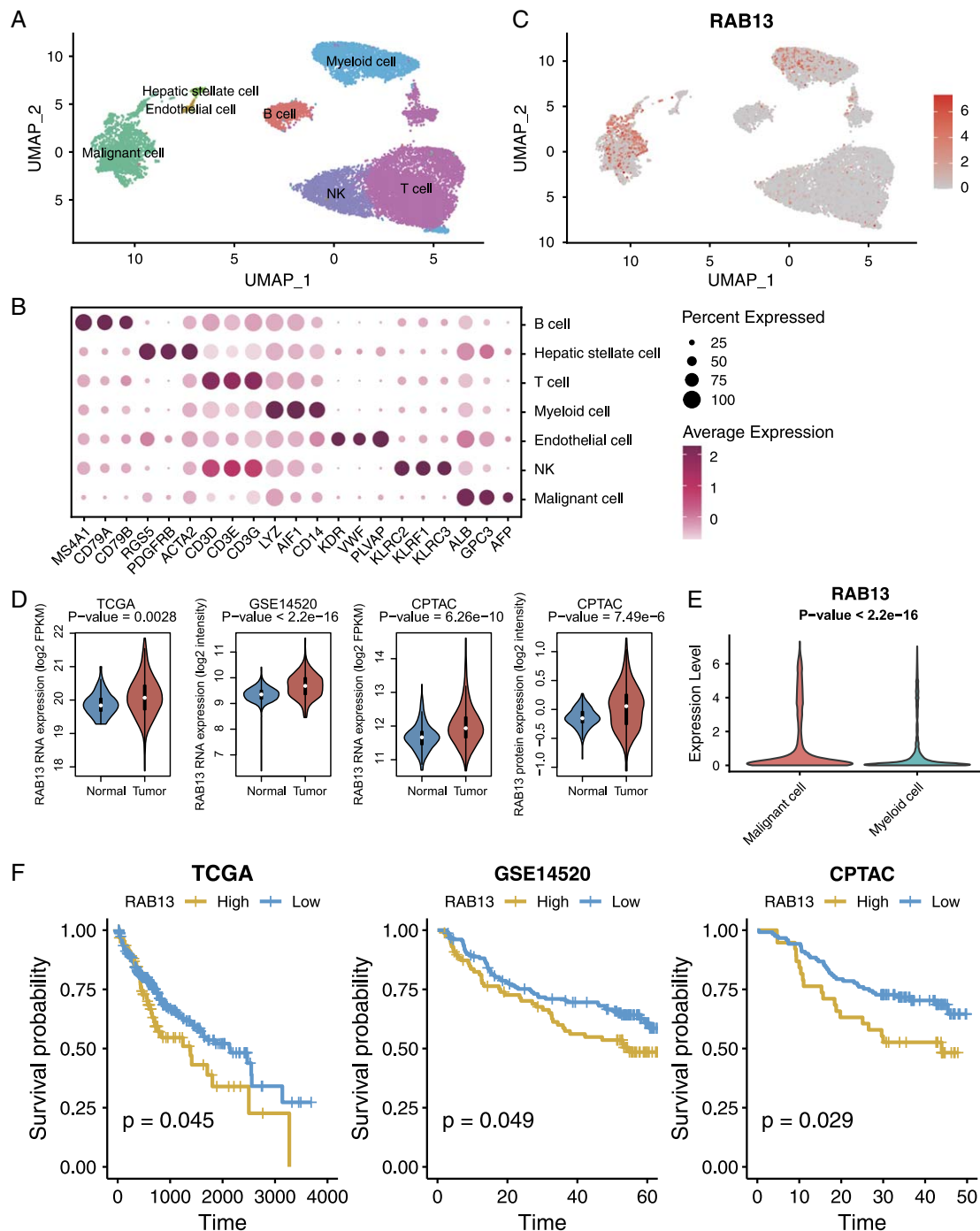
FIGURE 2 RAB13 RNA/protein expression levels in HCC malignant cells and tissues. (A) The cell annotation for the single-cell RNA sequencing data of HCC samples. (B) The differential expression levels of marker gene in the cell types of HCC tissues by single-cell RNA sequencing. The color represents the average expression and the diameter of the circle represents the percentage of expressed cells. (C) The RNA expression levels of RAB13 in the cell types of HCC tissues. (D) The differential RNA/protein expression levels of RAB13 between HCC tissues and adjacent normal tissues. (E) Differential RNA expression levels of RAB13 between malignant cells and myeloid cells in HCC tissues. (F) The prognostic value of RAB13 RNA expression in HCC.

[RAB13 overexpression (OE-RAB13) vs. control (Scramble-CON), 11.1 ± 2.9 vs. 8.3 ± 1.8, $p < 0.001$, Figure 3C].

Furthermore, we also employed the ELISA to detect the concentrations of MMP2 (ng/mL) and TIMP2 (ng/mL), the well-recognized biomarkers for cancer invasion, in the supernatant of MHCC97H cells with stable lentiviral transfection of si-NC or si-RAB13 (co-culture for 12, 24, 36, and 48 hours). Compared with si-NC group, si-RAB13 group had an unchanged expression of MMP2, but had an increased expression of TIMP2 and a decrease of the ratio of MMP2/TIMP2
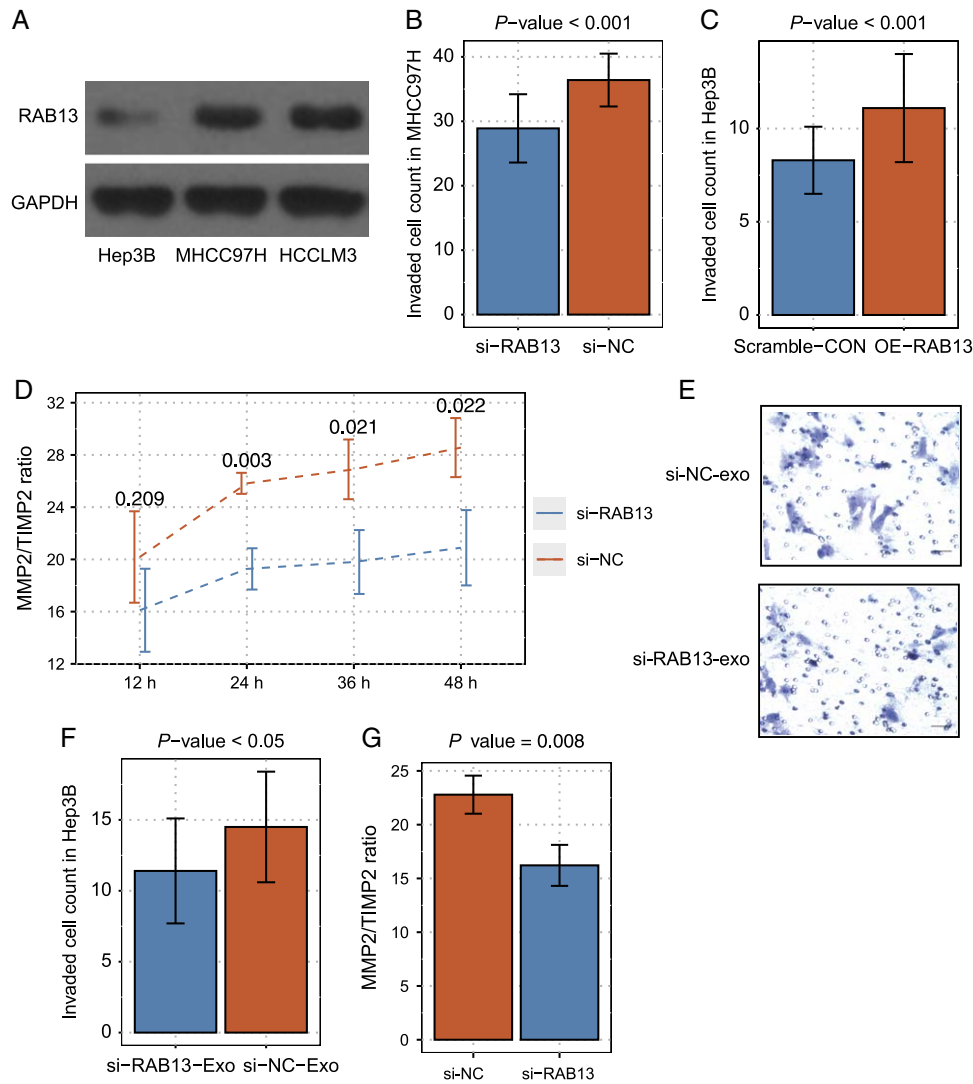
FIGURE 3   The impact of RAB13 on HCC invasion by *in vitro* study. (A) The protein expression of RAB13 in HCC cell lines by western blot. (B) The number of invaded cells in MHCC97H treated with si-NC or si-RAB13. (C) The number of invaded cells in Hep3B treated with and without RAB13 overexpression. (D) The differences of the MMP2/TIMP2 ratio between MHCC97H supernatants treated with si-NC and si-RAB13 across the 4 time points (12, 24, 36, and 48 hours). (E) The impact of MHCC97H derived si-NC-Exo or si-RAB13-Exo on Hep3B invasion by Transwell assay (*bar*, 50 μm). (F) The number of invaded cells in Hep3B treated with si-NC-Exo or si-RAB13-Exo. (G) MMP2/TIMP2 ratio in supernatants from Hep3B, which were co-cultured with exosomes derived from MHCC97H treated with si-NC and si-RAB13 after 24 hours (si-NC-Exo vs. si-RAB13-Exo).

(Figure 3D). Notably, the most significant changes of TIMP2 and the ratio of MMP2/TIMP2 were observed at 24 hours.

Subsequently, we also isolated the exosomes from culture supernatants of MHCC97H following our previous study[13] (Figure S3, http://links.lww.com/HC9/A11), and the Hep3B cells were co-cultured with the exosomes derived from MHCC97H with si-NC or si-RAB13 treatments after 24 hours. The number of invaded cells was greater in the Hep3B cells co-cultured with exosomes derived from MHCC97H of si-NC group (si-NC-Exo), as compared with si-RAB13 group (si-RAB13-Exo) (Figure 3E, F, si-RAB13-Exo vs. si-NC-Exo, 11.4 ± 3.7 vs. 14.5 ± 3.9, $p < 0.05$), respectively. Accordingly, the measurements of MMP2

and TIMP2 in the supernatants of Hep3B revealed that the MMP2/TIMP2 ratio was significantly decreased in si-RAB13-Exo as compared with si-NC-Exo (Figure 3G). These results suggested that RAB13 silence in HCC could attenuate the exosome-induced invasion.

RAB13 is associated with CTC accumulation and clustering, and HCC metastasis based on *in vivo* study and clinical samples

Considering that tumor-derived exosomes could promote metastasis by increasing CTC counts based on previous study,[15–17] we then investigated whether
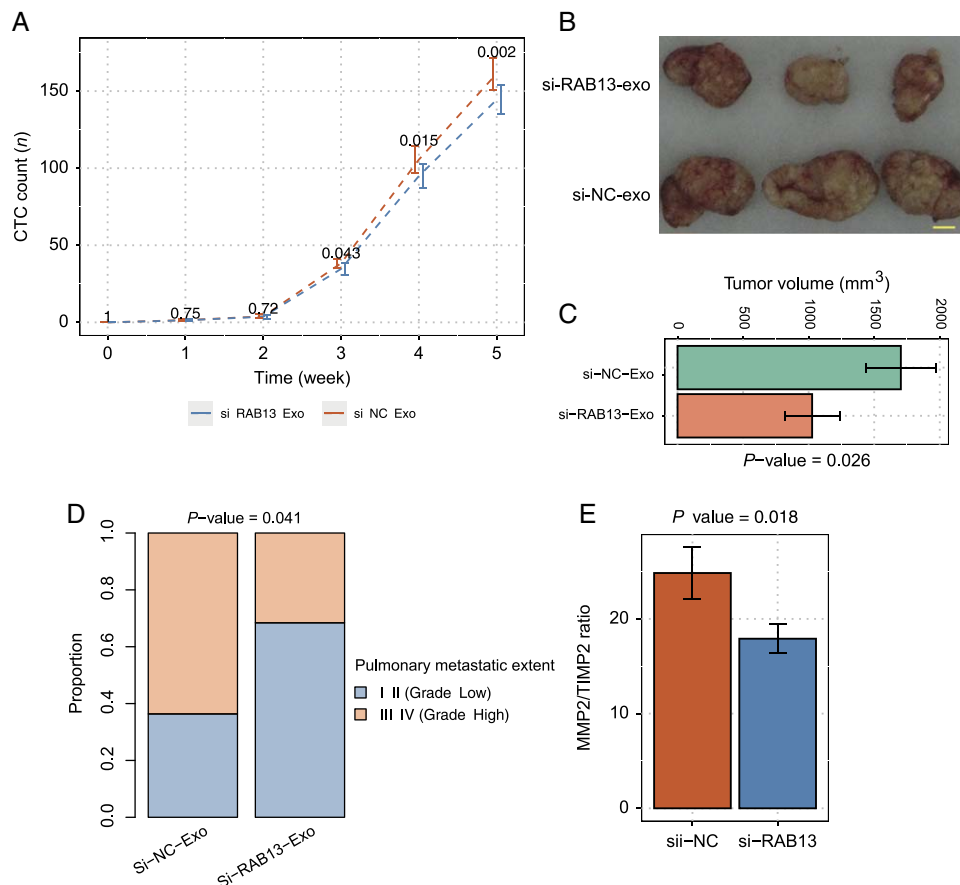
FIGURE 4 The impact of RAB13 on HCC metastasis by *in vivo* study. (A) The CTC counts between mouse models treated with si-NC-Exo or si-RAB13-Exo at 0, first, second, third, fourth, and fifth weeks. (B and C) The tumor sizes (*bar*, 5 mm) between mouse models treated with si-NC-Exo or si-RAB13-Exo. (D) The proportion of high-grade pulmonary metastatic nodules in si-NC-Exo or si-RAB13-Exo groups. (E) The difference of MMP2/TIMP2 ratio between supernatants from mouse models treated with si-NC-Exo or si-RAB13-Exo at fifth week.

RAB13 silence could inhibit tumor-derived exosomes-induced CTC accumulation/clustering and HCC metastasis by orthotopic mouse model of HCC. Specifically, we randomly divided the 36 mouse models into control ($n = 18$, si-NC-Exo) and treatment ($n = 18$, si-RAB13-Exo) groups by intravenous injection of 100 μg (1 μg/μL) exosomes derived from MHCC97H cell with si-NC and si-RAB13 through tail vein, respectively, following the methods of our previous work. To investigate the dynamic changes of CTCs, 3 nude mice in each group were sacrificed by neck dissection, and blood was collected from eyeballs to capture CTCs at weeks 0, 1, 2, 3, 4, and 5 after orthotopic transplantation of tumors. No significance differences of CTC counts were observed between si-NC-Exo and si-RAB13-Exo groups at 0, first and second weeks, while the CTC counts were decreased about 9.4% ($p = 0.043$), 10.1% ($p = 0.015$), and 10.5% ($p = 0.002$) in si-RAB13-Exo group as compared with si-NC-Exo group at third, fourth, and fifth weeks (Figure 4A). As shown in Figure 4B and C, the tumor volume (mm^3) was significantly greater in si-NC-Exo group than si-RAB13-Exo group (1703.2 ± 268.0 vs. 1026.6 ± 210.4, $p < 0.05$) at the end of the fifth week. Particularly, we

also observed CTC clusters were exclusively occurred at the fifth week. In addition, the proportion of high-grade lung metastatic nodule in si-NC-Exo group was higher than that in si-RAB13-Exo group (Figure 4D and Figure S4, http://links.lww.com/HC9/A12, Table 1, chi-square test, $p < 0.05$). In accordance with the *in vitro* findings, the ratio of MMP2/TIMP2 was significantly decreased in the mouse models of si-RAB13-Exo group as compared with si-NC-Exo group at the fifth week (Figure 4E, $p < 0.05$). These results indicated that silence of RAB13 could attenuate HCC metastasis.

We have previously proved that pulmonary metastasis was frequently observed at the fifth week in mouse models,[30,31] which was equivalent to the advanced stage of HCC. Therefore, we selected 10 consecutive cases with advanced HCC (TNM stage, IIIc–IV) that had been surgically removed recently (Table S1, http://links.lww.com/HC9/A15), including 6 cases with metastases (tumor thrombus in the main branch of portal vein is defined as intrahepatic metastasis) and 4 cases without any metastasis. The IHC for RAB13 indicated that the metastatic group had a higher RAB13 intensity than the nonmetastatic group

TABLE 1   Effects of HCC-derived exosomes on pulmonary metastasis

Group	The number of lung metastatic nodule (n)	Pulmonary metastatic extent (grade)	
		I–II (grade^Low)	III–IV (grade^High)
si-NC-Exo	22	8	14
si-RAB13-Exo	19	13	6

Lung metastases were verified by hematoxylin and eosin staining, and the difference of pulmonary metastatic extent between 3 groups was significantly ($p = 0.041$).

(Figure 5A). The imageological and pathological diagnosis for the primary HCC and metastatic lymph node of the representative case (case no. 2) could be seen in Figure S5 (http://links.lww.com/HC9/A13). The metastatic group had more preoperative CTC count than that in the nonmetastatic group (Figure 5B, 16.5 ± 2.7 vs. 14.1 ± 2.8, $p = 0.024$). Moreover, we also captured the CTCs in peripheral blood 3 times in 1 week before surgery or transcatheter arterial chemoembolization for each patient, and observed that the CTC clusters were more frequently observed in metastatic group than the nonmetastatic group (Figure 5C, 12/18 vs. 2/12, $p = 0.011$). Moreover, the 10 patients were divided into RAB13 high ($n = 5$) and low groups ($n = 5$) (RAB13-hi vs. RAB13-lo) based on the RAB13 protein expression by IHC assay. The RAB13-hi group had a higher percentage of metastasis than the RAB13-lo group (4/5 vs. 2/5). The RAB13-hi group had 19.8% CTC count more than the RAB13-lo group (Figure 5D, $p = 0.007$). In addition, the frequency of CTC clusters in RAB13-hi group is 3.7 times as that in RAB13-lo group (Figure 5E, $p = 0.009$). These results indicated that RAB13 was closely associated with HCC metastasis.

RAB13 promotes angiogenesis via upregulating VEGF in HCC

To further investigate the impact of RAB13 on the TME, we divided the HCC samples in the scRNA-seq dataset into RAB13-hi and RAB13-lo groups based on their average expression of RAB13 in malignant cells. Among the cell types annotated by scRNA-seq data, the proportion of endothelial cells was higher in RAB13-hi group than RAB13-lo group (Figure 6A, $p < 0.05$). The vascular endothelial cell markers, such as *VWF*, *KDR*, and *NRP1/2*, had higher expression levels in RAB13-hi group (Figure 6B, $p < 0.05$). Notably, both RAB13-hi malignant cells and RAB13-hi HCC cell models had a higher expression level of VEGFA (Figure 6C, $p < 0.05$), suggesting that RAB13-hi malignant cells might promote angiogenesis by overexpression of VEGFA. Furthermore, a deconvolution method was employed to estimate the cell proportions in HCC tissues using bulk RNA sequencing data, and RAB13 expression was positively correlated with endothelial cell

proportion in HCC tissues (Figure 6D, Spearman correlation, $p < 0.05$). *In vitro*, the measurement of VEGF in the supernatants of Hep3B co-cultured with exosomes from MHCC97H revealed that the VEGF expression was significantly decreased in si-RAB-13-Exo as compared with si-NC-Exo (Figure 6E). The cell proliferation assay of the HUVECs co-cultured with exosomes derived from MHCC97H revealed that RAB13 silence significantly suppress the cell proliferation of HUVECs (Figure 6F). Accordingly, tube formation assay revealed that the tube formation in si-RAB13-Exo group was significantly inhibited as compared with the si-NC-Exo group (Figure 6G). *In vivo*, VEGF protein level was significantly decreased in the mouse models of si-RAB13-Exo group as compared with si-NC-Exo group at the fifth week (Figure 6H, $p < 0.05$). In addition, the microvessel density analysis of the orthotopic mouse model of HCC revealed that si-RAB13-Exo group had a significant lower MVD than si-NC-exo group (Figure 6I, J, 42.9 ± 5.2 vs. 38.1 ± 4.4, $p < 0.05$). These results indicated that RAB13 was associated with angiogenesis in HCC.

In silico analysis reveals RAB13 is involved in vesicle-mediated transport through CUX1 in HCC cells

To further infer the molecular mechanism of RAB13 underlying HCC metastasis, we compared the malignant cells of high RAB13 expression (RAB13-hi) with those of low RAB13 expression (RAB13-lo) using the scRNA-seq data. The genes upregulated in RAB13-hi malignant cells were significantly enriched in vesicle-mediated transport, membrane trafficking, G2M checkpoint, ECM organization, hypoxia, cell cycle, degradation of the ECM, and translocation of SLC2A4 (GLUT4) to the plasma membrane (Figure 7A). As RAB13 was involved in vesicle-mediated transport, the key components in this pathway, such as *VPS45*, *KIFAP3*, *CUX1*, *YWHAG*, *CD55*, *EXOC2*, *TJP1*, *CCZ1*, *NECAP1*, *TUBA1B*, *COL4A2*, *KIF1B*, *STX4*, and *COPS2*, were expressed higher in RAB13-hi than RAB13-lo malignant cells (Figure 7B). Moreover, we also investigated the expression levels of those genes in 79 HCC cell models from the previous study.[32] Consistently, those genes were also upregulated in
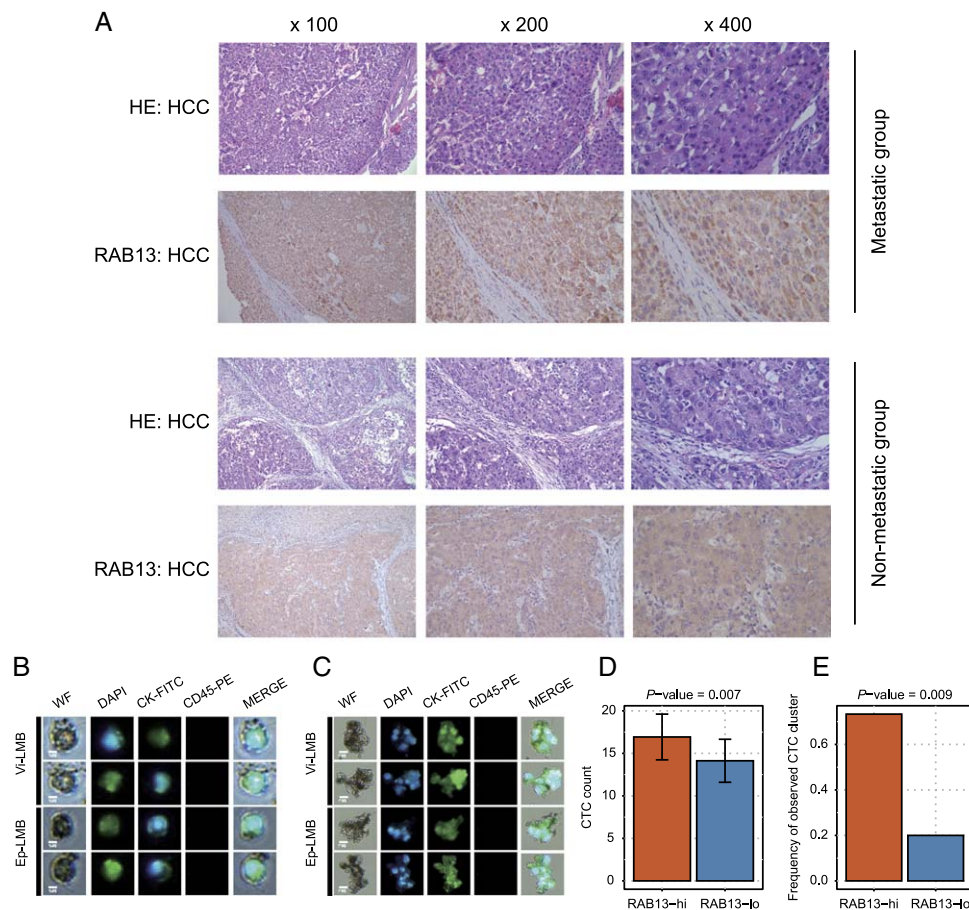
FIGURE 5 Hematoxylin and eosin (HE) staining and immunohistochemistry for RAB13 in primary HCC tissues of metastatic and non-metastatic groups and the scanning electron microscopy of circulating tumor cells (CTCs) and CTC clusters. (A) The HE staining and immunohistochemistry for RAB13 in the primary HCC tissues of metastatic and nonmetastatic groups (original magnifications: ×100, ×200, and ×400). (B) Immunofluorescent identification of single CTCs in HCC patients. (C) Immunofluorescence identification of CTC clusters (Captured by Ep-LMB and Vi-LMB, respectively, and identified by immunofluorescence by DAPI, CK-FITC, and CD45-PE). (D) The CTC counts in HCC patients of RAB13-hi and RAB13-lo groups. (E) The percentages of CTC clusters observed in HCC patients of RAB13-hi and RAB13-lo groups.

RAB13-hi cell models as compared with RAB13-lo cell models (Figure 7C, $p < 0.05$). RAB13 was directly connected with *CUX1*, *STX4*, *EXOC2*, *TJP1*, and *YWHAG* by mapping those genes to protein-protein interaction network, of which, *CUX1*, encoding a transcription factor, might act as one of the downstream effectors of *RAB13* (Figure 7D). The gene set enrichment analysis revealed that CUX1 target genes were significantly enriched in the upregulated genes of RAB13-hi group (false discovery rate < 0.05, Figure 7E). These results indicated that RAB13 was associated with enhanced vesicle-mediated transport capability and transcriptional activity of CUX1 in HCC cells.

DISCUSSION

Tumor-derived exosomes contain abundant proteins, and exosomal proteins from cancer cells are becoming new biomarkers for cancer monitoring and efficacy evaluation.[33] However, their biological function and molecular mechanism underlying tumor metastasis are largely unknown. In this study, we conducted a systematically bioinformatic analysis to screen out RAB13 as one of the critical regulators of HCC metastasis in tumor-derived exosomes for the first time. RAB13 was observed to be upregulated in HCC cell lines with highly metastatic potential, and its RNA was specifically expressed in malignant cells by scRNA-seq data. The transcriptome and proteome analysis revealed that RAB13 RNA and protein expression levels were upregulated in HCC tissues as compared with the adjacent normal tissues, and its high expression was associated with worse prognosis, indicating that RAB13 was closely associated with HCC progression. Rab13, whose subcellular localization sites include recycling endosome, tubular endosome, trans-Golgi network and tight junction, belongs to the Rab8/Sec. 4 subfamily.[34] Rab13 is capable of disrupt tight junction assembly via
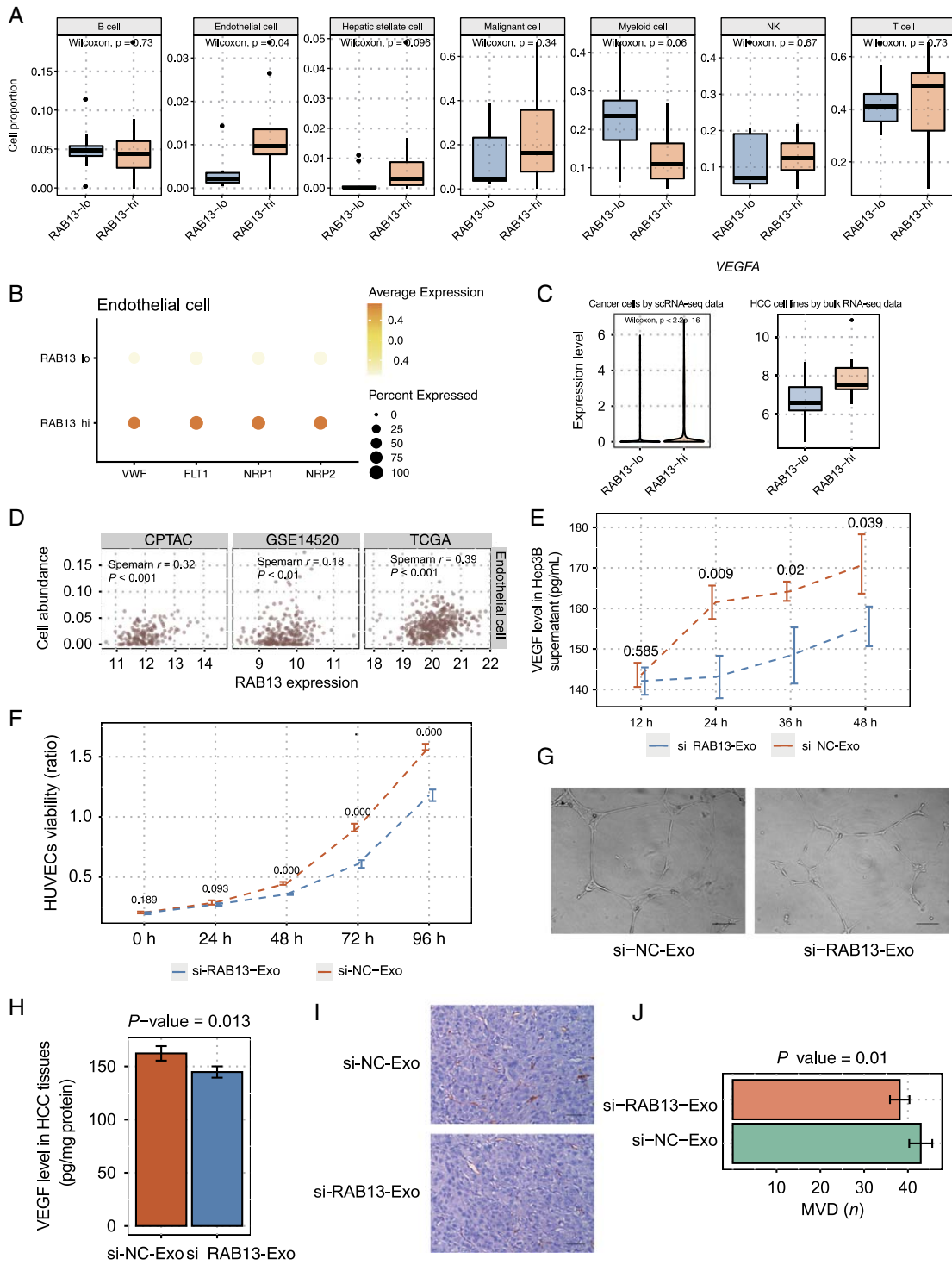
FIGURE 6 The association of RAB13 with angiogenesis in HCC. (A) The differential cell proportions between RAB13-hi and RAB13-lo HCC samples by single-cell RNA sequencing data. (B) The expression of vascular endothelial markers in RAB13-hi and RAB13-lo endothelial cells. (C) The differential expression levels of VEGFA expression between RAB13-hi and RAB13-lo malignant cells (left) and HCC cell lines (right). (D) The correlation between RAB13 expression and endothelial cell proportion in HCC tissues by bulk RNA sequencing data. (E) The VEGF levels in MHCC97H supernatants treated with si-NC and si-RAB13 across the 4 time points (12, 24, 36, and 48 hours). (F) The CCK8 assay for the proliferation of human umbilical vein endothelial cells co-cultured with exosomes derived from MHCC97H with (si-RAB13-Exo group) and without (si-NC-Exo group) RAB13 silence. (G) The tube formation assay for the human umbilical vein endothelial cells co-cultured with exosomes derived from MHCC97H with (si-RAB13-Exo group) and without (si-NC-Exo group) RAB13 silence. (H) Tumor VEGF levels in mouse models (si-RAB13-Exo vs. si-NC-Exo groups) at fifth week. (I) Representative CD34 immunostained intratumoral microvessels of si-RAB13-Exo and si-NC-Exo groups (original magnification, ×200; *bar*, 50 μm). (J) The MVD count in HCC tissues of mouse models (si-RAB13-Exo vs. si-NC-Exo groups).
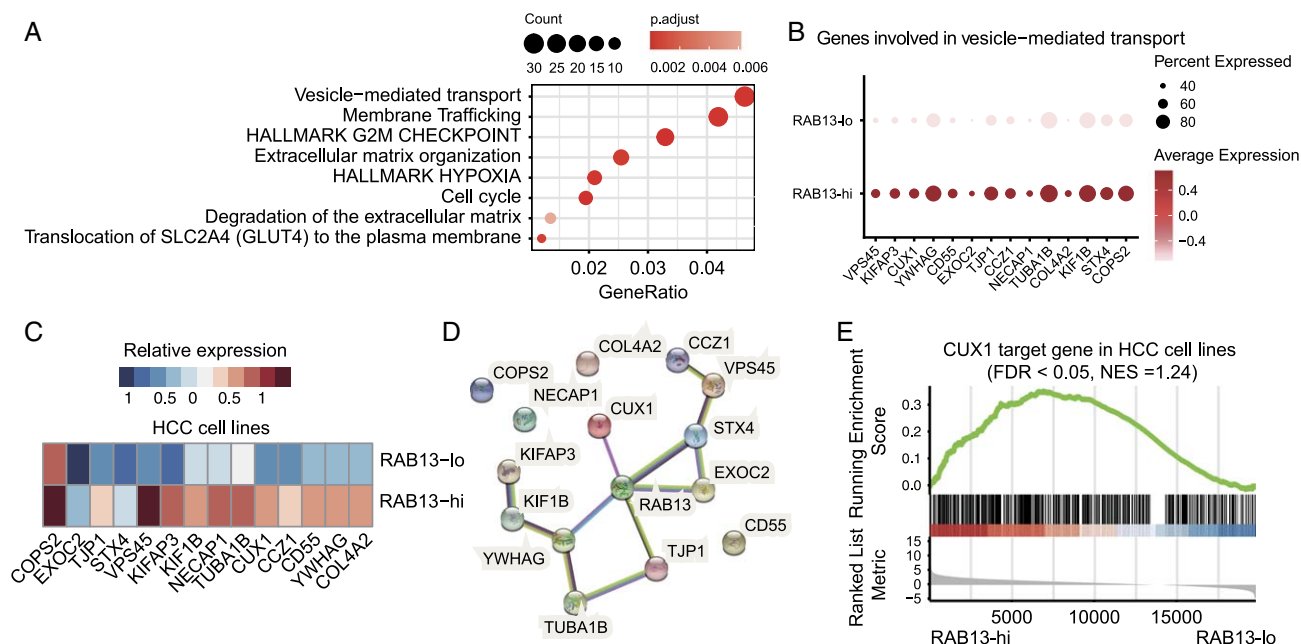
FIGURE 7 The inference of RAB13 downstream pathways. (A) The pathways enriched by the upregulated genes in the RAB13-hi malignant cells. (B) The differential expression levels of key components involved in vesicle-mediated transport between RAB13-hi and RAB13-lo malignant cells. (C) The differential expression levels of key components involved in vesicle-mediated transport between RAB13-hi and RAB13-lo cell models. (D) The protein-protein interaction (PPI) network of the key components involved in vesicle-mediated transport. (E) CUX1 target genes significantly enriched in RAB13-hi cell models.

binding to PKA, which in turns enhances the invasiveness of malignant cells.[35]

In vitro, the invasiveness of Hep3B cells co-cultured with the exosomes derived from MHCC97H was significantly attenuated by silencing RAB13 in MHCC97H, and the Hep3B cells had a decreased ratio of MMP2/TIMP2 expression in the supernatants, suggesting that exosomes with RAB13 silence could attenuate the HCC invasion. Consistently, RAB13 has been reported to regulate small extracellular vesicles secretion in mutant KRAS colorectal cancer cells, and mediate cell proliferation and invasion *via* autocrine and paracrine signaling.[36] *In vivo*, CTC counts were decreased about 9.4% ($p = 0.043$), 10.1% ($p = 0.015$), and 10.5% ($p = 0.002$) in si-RAB13-Exo group as compared with si-NC-Exo group at third, fourth, and fifth weeks after orthotopic transplantation of tumors, suggesting that RAB13 silence could efficiently reduce the tumor burden, which may be attributed to the decline of the MMP2/TIMP2 ratio. Furthermore, larger tumor size, higher proportion of high-grade lung metastatic nodule, and higher expression of MMP2/TIMP2 ratio were observed in si-NC-Exo group, as compared with si-RAB13-Exo group, further indicating that *RAB13* silence could reduce HCC metastasis. In addition, the HCC patients with higher RAB13 expression had more CTC counts and higher detectable rates of CTC clusters, suggesting that RAB13 were closely associated with HCC metastasis.

Furthermore, we also found that the proportion of endothelial cells was higher in RAB13-hi group than RAB13-lo group by scRNA-seq data. The vascular endothelial cell markers, such as VWF, KDR, and NRP1/2 had higher expression levels in RAB13-hi group, and both RAB13-hi malignant cells and RAB13-hi HCC cell models had a higher expression level of VEGFA, suggesting that RAB13-hi malignant cells might promote angiogenesis by overexpression of VEGFA. Besides, the VEGF level in both *in vitro* and *in vivo* models was positively correlated with RAB13 expression. The co-culture of HUVECs with the exosomes derived from MHCC97H suggested that RAB13 silence could significantly suppress HUVECs proliferation and tube formation. *In vivo*, MVD analysis of the orthotopic mouse model of HCC revealed that si-RAB13-Exo group had a significant lower MVD than si-NC-Exo group, indicating that RAB13 was associated with angiogenesis in HCC. Consistently, RAB13 has been shown to play a role in angiogenesis.[37,38]

In addition, we also explored the underlying mechanism of RAB13 in HCC metastasis. RAB13 was predicted to regulate in vesicle-mediated transport through CUX1. In addition to regulating vesicle-mediated membrane trafficking, CUX1 could also increase tumor cell proliferation, tumor growth, resistance to apoptosis, and angiogenesis *in vitro* and *in vivo* in pancreatic neuroendocrine neoplasms.[39]

However, the present work is a preliminary study and has some limitations. First, the detailed molecular mechanism of metastasis driven by exosomal RAB13 is still unclear. Second, the clinical significance of exosomal RAB13 needs further validation. In conclusion, we systematically analyzed multiomic data to screen out RAB13 as a key regulator of HCC metastasis in exosomes, demonstrated its functional role, and inferred its molecular mechanism underlying HCC metastasis, which improved our understanding of exosomal protein-mediated HCC metastasis.

AUTHOR CONTRIBUTIONS

X.-Ya.H., Z.-L.H., J.Z., and Z.-Y.T. designed and coordinated the study. X.-Ya.H., Z.-L.H., F.L., T.-T.L., J.-T.Z., and J.H. performed the experiments, acquired, and analyzed data. X.-J.S. and X.-Yu.H. prepared clinical data. X.-Ya.H., Z.-L.H., F.L., X.-J.S., J.H., and X.-Yu.H. interpreted the data. X.-Ya.H., Z.-L.H., and F.L. wrote the manuscript. J.Z. and Z.-Y.T. reviewed and edited the manuscript. All authors approved the final version of the article.

ACKNOWLEDGMENTS

CONFLICT OF INTEREST

ORCID

Xiu-Yan Huang https://orcid.org/0000–0002–6416–9281
Jun-Tao Zhang https://orcid.org/0000–0002–4069–5164
Feng Li https://orcid.org/0000–0002–5594–7387
Ting-Ting Li https://orcid.org/0000–0001–9680–7260
Xiang-Jun Shi http://https://orcid.org/0000–0002–9827–694X
Jin Huang https://orcid.org/0000–0001–8009–7831
Xin-Yu Huang https://orcid.org/0000–0002–4802–1172
Jian Zhou https://orcid.org/0000–0001–7482–2072
Zhao-You Tang https://orcid.org/0000–0001–9776–2623
Zi-Li Huang https://orcid.org/0000–0001–6733–3887

REFERENCES

1. Sung H, Ferlay J, Siegel RL, Laversanne M, Soerjomataram I, Jemal A, et al. Global Cancer Statistics 2020: GLOBOCAN estimates of incidence and mortality worldwide for 36 cancers in 185 countries. CA Cancer J Clin. 2021;71:209–49.
2. Sas Z, Cendrowicz E, Weinhauser I, Rygiel TP. Tumor micro-environment of hepatocellular carcinoma: challenges and opportunities for new treatment options. Int J Mol Sci. 2022;23:3778.
3. Choi J, Gyamfi J, Jang H, Koo JS. The role of tumor-associated macrophage in breast cancer biology. Histol Histopathol. 2018;33:133–45.
4. Deepak KGK, Vempati R, Nagaraju GP, Dasari VR, N S, Rao DN, et al. Tumor microenvironment: challenges and opportunities in targeting metastasis of triple negative breast cancer. Pharmacol Res. 2020;153:104683.
5. Dominiak A, Chelstowska B, Olejarz W, Nowicka G. Communication in the cancer microenvironment as a target for therapeutic interventions. Cancers (Basel). 2020;12:1232.
6. Giannelli G, Bergamini C, Marinosci F, Fransvea E, Quaranta M, Lupo L, et al. Clinical role of MMP-2/TIMP-2 imbalance in hepatocellular carcinoma. Int J Cancer. 2002;97:425–31.
7. Di Martino JS, Akhter T, Bravo-Cordero JJ. Remodeling the ECM: implications for metastasis and tumor dormancy. Cancers (Basel). 2021;13:4916.
8. Fevrier B, Raposo G. Exosomes: endosomal-derived vesicles shipping extracellular messages. Curr Opin Cell Biol. 2004;16:415–21.
9. Kalluri R, LeBleu VS. The biology, function, and biomedical applications of exosomes. Science. 2020;367:6478.
10. Wu Q, Zhou L, Lv D, Zhu X, Tang H. Exosome-mediated communication in the tumor microenvironment contributes to hepatocellular carcinoma development and progression. J Hematol Oncol. 2019;12:53.
11. Kok VC, Yu CC. Cancer-derived exosomes: their role in cancer biology and biomarker development. Int J Nanomedicine. 2020;15:8019–36.
12. Kalluri R. The biology and function of exosomes in cancer. J Clin Invest. 2016;126:1208–15.
13. Huang XY, Huang ZL, Huang J, Xu B, Huang XY, Xu YH, et al. Exosomal circRNA-100338 promotes hepatocellular carcinoma metastasis via enhancing invasiveness and angiogenesis. J Exp Clin Cancer Res. 2020;39:20.
14. Han B, Zhang H, Tian R, Liu H, Wang Z, Wang Z, et al. Exosomal EPHA2 derived from highly metastatic breast cancer cells promotes angiogenesis by activating the AMPK signaling pathway through Ephrin A1-EPHA2 forward signaling. Theranostics. 2022;12:4127–46.
15. Fu Q, Zhang Q, Lou Y, Yang J, Nie G, Chen Q, et al. Primary tumor-derived exosomes facilitate metastasis by regulating adhesion of circulating tumor cells via SMAD3 in liver cancer. Oncogene. 2018;37:6105–18.
16. Hoshino A, Costa-Silva B, Shen TL, Rodrigues G, Hashimoto A, Tesic Mark M, et al. Tumour exosome integrins determine organotropic metastasis. Nature. 2015;527:329–35.
17. Ozimski LL, Gremmelspacher D, Aceto N. A fatal affair: circulating tumor cell relationships that shape metastasis. iScience. 2021;24:103073.
18. Wang H, Xu H, Chen W, Cheng M, Zou L, Yang Q, et al. Rab13 sustains breast cancer stem cells by supporting tumor-stroma cross-talk. Cancer Res. 2022;82:2124–40.
19. Huang XY, Wang L, Huang ZL, Zheng Q, Li QS, Tang ZY. Herbal extract "Songyou Yin" inhibits tumor growth and prolongs survival in nude mice bearing human hepatocellular carcinoma xenograft with high metastatic potential. J Cancer Res Clin Oncol. 2009;135:1245–55.
20. Zhang J, Lu S, Zhou Y, Meng K, Chen Z, Cui Y, et al. Motile hepatocellular carcinoma cells preferentially secret sugar metabolism regulatory proteins via exosomes. Proteomics. 2017;17:13–4.
21. Ma L, Hernandez MO, Zhao Y, Mehta M, Tran B, Kelly M, et al. Tumor cell biodiversity drives microenvironmental reprogramming in liver cancer. Cancer Cell. 2019;36:418–430 e416.
22. Hao Y, Hao S, Andersen-Nissen E, Mauck WM III, Zheng S, Butler A, et al. Integrated analysis of multimodal single-cell data. Cell. 2021;184:3573–587 .e3529.
23. Korsunsky I, Millard N, Fan J, Slowikowski K, Zhang F, Wei K, et al. Fast, sensitive and accurate integration of single-cell data with Harmony. Nat Methods. 2019;16:1289–96.

24. Wang X, Park J, Susztak K, Zhang NR, Li M. Bulk tissue cell type deconvolution with multi-subject single-cell expression reference. Nat Commun. 2019;10:380.

25. Wu T, Hu E, Xu S, Chen M, Guo P, Dai Z, et al. clusterProfiler 4.0: A universal enrichment tool for interpreting omics data. Innovation (Camb). 2021;2:100141.

26. Liu Y, Li Q, Chen T, Shen T, Zhang X, Song P, et al. Clinical verification of vimentin/EpCAM immunolipid magnetic sorting system in monitoring CTCs in arterial and venous blood of advanced tumor. J Nanobiotechnology. 2021;19:185.

27. Weidner N, Semple JP, Welch WR, Folkman J. Tumor angiogenesis and metastasis–correlation in invasive breast carcinoma. N Engl J Med. 1991;324:1–8.

28. Giordano S, Columbano A. Met as a therapeutic target in HCC: facts and hopes. J Hepatol. 2014;60:442–52.

29. You H, Ding W, Dang H, Jiang Y, Rountree CB. c-Met represents a potential therapeutic target for personalized treatment in hepatocellular carcinoma. Hepatology. 2011;54:879–89.

30. Li Y, Tang ZY, Ye SL, Liu YK, Chen J, Xue Q, et al. Establishment of cell clones with different metastatic potential from the metastatic hepatocellular carcinoma cell line MHCC97. World J Gastroenterol. 2001;7:630–6.

31. Li Y, Tang Y, Ye L, Liu B, Liu K, Chen J, et al. Establishment of a hepatocellular carcinoma cell line with unique metastatic characteristics through in vivo selection and screening for metastasis-related genes through cDNA microarray. J Cancer Res Clin Oncol. 2003;129:43–51.

32. Qiu Z, Li H, Zhang Z, Zhu Z, He S, Wang X, et al. A pharmacogenomic landscape in human liver cancers. Cancer Cell. 2019;36:179–193 .e111.

33. Li W, Li C, Zhou T, Liu X, Liu X, Li X, et al. Role of exosomal proteins in cancer diagnosis. Mol Cancer. 2017;16:145.

34. Homma Y, Hiragi S, Fukuda M. Rab family of small GTPases: an updated view on their regulation and functions. FEBS J. 2021; 288:36–55.

35. Ioannou MS, McPherson PS. Regulation of cancer cell behavior by the small GTPase Rab13. J Biol Chem. 2016;291:9929–37.

36. Hinger SA, Abner JJ, Franklin JL, Jeppesen DK, Coffey RJ, Patton JG. Rab13 regulates sEV secretion in mutant KRAS colorectal cancer cells. Sci Rep. 2020;10:15804.

37. Wu C, Agrawal S, Vasanji A, Drazba J, Sarkaria S, Xie J, et al. Rab13-dependent trafficking of RhoA is required for directional migration and angiogenesis. J Biol Chem. 2011;286:23511–20.

38. Xie Y, Mansouri M, Rizk A, Berger P. Regulation of VEGFR2 trafficking and signaling by Rab GTPase-activating proteins. Sci Rep. 2019;9:13342.

39. Krug S, Kuhnemuth B, Griesmann H, Neesse A, Muhlberg L, Boch M, et al. CUX1: a modulator of tumour aggressiveness in pancreatic neuroendocrine neoplasms. Endocr Relat Cancer. 2014;21:879–90.